Estimating reflectance property from refocused images and its application to auto material appearance balancing

Norimichi Tsumura[1)], Kaori Baba[1)], Shoji Yamamoto[2)], and Masao Sambongi[3)]

1) Graduate School of Advanced Integration Science,
Chiba University
1-33 Yayoi-cho, Inage-ku, Chiba-shi, Chiba 263-8522, Japan
tsumura@faculty.chiba-u.ac.jp

2) Tokyo Metropolitan College of Industrial Technology
8-17-1 Minamisenjyu, Arakawa-ku, Tokyo 116-0003, Japan

3) Olympus Corporation,
2-3 Kuboyama-cho, Hachiouji-shi, Tokyo 192-8512, Japan

A portion of this paper was presented at the IS&T/SPIE EI2015 conference held in San Francisco.

Abstract

In this paper, we propose a method to estimate the reflectance property from refocused images from a light source reflected on an object. The blurred information of the light source on the surface of the object is expected to be a practical method to estimate the reflectance property, although various methods have already been proposed. Because the degree of blurred information is changed with the position of focus in the camera, we introduce a light field camera that can change the position of focus after the image is captured. In this research, we chose the refocused image where the light source is focused through the reflection on the object surface. Based on the blurred information of the focused light source, we estimate the reflectance property of the object. The estimated reflectance property is applied to inverse rendering for auto material appearance balancing.

Keywords: reflectance property, SR-PSF, inverse rendering, auto material appearance balancing

1. Introduction

We are surrounded by various light sources, and the detected color of an object changes with the changes of these light sources. Humans can perceive the same color under a light source of arbitrary color by color constancy [1-3]. However, the correct color cannot be perceived when an image of an object is taken by a camera and observed under different illuminants. Therefore, some digital cameras have an auto white balancing function to estimate the color of the light source and to compensate the color of an image under a standard light source. Based on this estimation, we can appropriately reproduce the color of an object under a different light source.

We are also surrounded by various shapes of light sources. The shape of specular reflection on an object changes with the changing shape of the light source. Humans can perceive the reflectance property correctly under various shapes of light sources [4]. However, it becomes difficult to perceive the reflectance property correctly when the captured image is observed under different shapes of light sources. Therefore, it is necessary to reproduce the material appearance of the reflectance property under different shapes of light sources based on the estimation of the reflectance property. This technique is known as the auto material appearance balancing function.

For acquiring the reflectance property, various studies have been performed in the field of computer vision and computer graphics [5-25]. In these studies, gloss is observed around the angle of specular reflection. To record this property, it is necessary to measure the reflectance by changing the incident and existent angles. Generally, a digital camera is used as a sensor, and a small light is used as a light source for this measurement. However, this method requires dense sampling, and the size of the instruments and the amount of the measurement time are large. Therefore, this is a difficult method for practical use [5-19]. To address this problem, a simple method has been proposed by limiting the object to a known shape and a homogeneous reflectance property [20-25]. Inoue et al. proposed the measurement of the specular reflection point spread function (SR-PSF) by using a single image [23-25]. Wang et al. also proposed the measurement of the blurriness of a light source image[22]. In the method of Wang et al., step-edge lighting is performed by displaying a white and black pattern [22]. The reflectance property is estimated from the degree of blurriness of the edge pattern.

As mentioned above, from the point of practical use, it would be effective to use the blurriness of the

shape of specular reflection, which is the image of the shape of the light source. However, in a general imaging condition, the blurriness depends on the position of the camera focus, as shown in Fig. 1. In Fig. 1, we can see that the shape of the specular reflection patterns is changed depending on the position of focus. Especially, in the high-gloss object, the degree of blurriness is strongly changed by the position of focus. Therefore, it is difficult to estimate the reflectance property from the general imaging condition.

In this paper, we propose to use a light field camera that can re-focus the image after taking the image for estimating the reflectance property. Since the light field camera can reproduce the light field in a single captured image, we can obtain the refocused image by a simple calculation in the captured image [26-33]. We use the light field camera to estimate the reflectance property by choosing the image where the light source is focused on the object. We also performed gloss reproduction under different lighting conditions based on this analysis as the auto material appearance balance function.

2. Measurement of SR-PSF

2.1 Measurement method

In this research, we use the specular reflection point spread function (SR-PSF) [23-25]. The point spread function is often used in the image processing field [28,29] and is applied to the specular reflection in SR-PSF. Figure 2 shows the apparatus we used to measure the SR-PSF for the present study. Light from a pinhole light source is projected onto sample paper through a collimator lens system. The light reflected from the sample paper is focused, and a two-dimensional charge-coupled device (CCD) camera captures a digital image of the intensity distribution of the reflected light. The camera is monochromatic camera with 14 bits values at each pixel. The camera can output linear values to the incoming light intensity. The captured image of the intensity distribution shows the SR-PSF of the sample because it is an impulse response to the pinhole light. SR-PSF has been applied in the printing industry [36, 37] as was the conventional point spread function of paper [34,35].

In this research, SR-PSF is measured for six kinds of flat surfaces that have different glossiness. Figure 3 shows the measured results of the samples. In the measured SR-PSFs, the peak value is decreased and the distribution is wider in the order of (a), (b), (c), (d), (e), (f). This is because the roughness of the object becomes larger in the same order; this result indicates that the light source image

is blurred on the object depending on the degree of roughness.

In this paper, we performed fitting to the approximation function for parameterization of the SR-PSF. As shown in Fig. 4, the shape of SR-SPF is sharper than a normal distribution function. Therefore, we checked other order of exponential function, then we found that simple exponential function is appropriate for the fitting. In this research, Equation (1) is used in the fitting. The maximum value is normalized to be one. Parameter a decides the slope of the function.

$$PSF_{SR}(y) = \frac{2}{a}\exp(-a\,|\,y\,|)\;\; a > 0 \qquad (1)$$

Figure 5 shows the values of parameter a for each sample. The difference of reflectance properties can be expressed by this single parameter.

3. Estimation of SR-PSF

3.1 Method

In this research, the reflectance property is estimated by assuming that an edge exists in the light source, as shown on the right-hand side in Fig. 6. As shown in Fig. 7, the edge of the light source image is blurred by the SR-PSF caused by the surface roughness and the PSF caused by the defocus. In the case of the light field camera, the focused image to an arbitrary position can be produced, as shown in the lower part in Fig. 7. Then, it is possible to reproduce the image focused on the light source on the object surface. The image is not expected to be influenced by the PSF caused from the defocus. From the blurriness of this focused edge, it is expected that the SR-PSF can be estimated.

Figure 8 shows the experimental system to confirm this principle. In this experiment, we used the computer monitor as the light source. The edge pattern is displayed in this experiment. The surface of the sample is illuminated by the edge pattern of the display. The sample is captured by the light field camera, Lytro. Refocused images are produced from the captured raw image. After pre-processing, which includes removal of the unevenness of intensity and noise, the image that is focused on the light source is selected from the multi-focus images. The detail of pre-processing is the same as that in reference [22]. By using this image, the reflectance property is estimated. Figure 9 shows an example of the edge slopes at various positions of focus. The maximum value of the slope is shown by the red arrow in Fig. 9. In this

maximum value of the gradient, we expect that the influence of defocus by the imaging system is negligible.

We consider that the light source is focused in the image where the gradient of the edge is the maximum. In the images shown in Fig. 10, the PSF caused from defocus to the light source is ignored, and the edge is considered to be blurred only by the SR-PSF. The reflectance property can be calculated by this blurriness. The shape of the light source is expressed by Equation (2) in this research, since we assumed that the edge is a part of the light source.

$$e(x) = \begin{cases} 1, & x \geq 0 \\ 0, & x < 0 \end{cases} \qquad (2)$$

The observed image $I(x)$ for the light source is calculated by Equation (3) by convolving between the edge and SR-PSF.

$$\begin{aligned} I(x') &= \int_{-\infty}^{\infty} PSF_{SR}(x' - x)e(x)dx \\ &= \int_{0}^{\infty} PSF_{SR}(x' - x)dx \\ &= \int_{0}^{x'} PSF_{SR}(x'')dx'' \end{aligned} \qquad (3)$$

where $x'' = x' - x$. From Equation (3), the integration of SR-PSF is the observed value $I(x)$. Then, by derivation of the observed value I, we obtain the SR-PSF as follows.

$$PSF_{SR}(x') = \frac{dI(x')}{dx'} \qquad (4)$$

From Equation (1), the derivative value of observed intensity I is related to parameter a in proportion, as follows.

$$PSF_{SR}(0) = \frac{2}{a} \qquad (5)$$

3.2 Results

Figure 11 shows the results of the estimation of the six kinds of samples. Each value is normalized by black glass. From this result, the estimated and measured values are matched when parameter a is large, which indicates the high-gloss samples, but are not matched in the low-gloss samples. This is because the surface roughness is high in the low-gloss samples. However, for the application of gloss reproduction, parameter a does not have a large influence on the low-gloss samples. Therefore, in this research, we use this estimated method for gloss reproduction.

4. Simulation of gloss

4.1 Method

Figure 12 shows the flow of the proposed method. First, the reflectance property is estimated from the refocused images. The object is illuminated by a light source where the edge is included. Next, SR-PSF is recovered based on the estimated reflectance parameter a in Equation (1). Next, by convolving the SR-PSF to a new shape of light source, we can obtain the new specular reflection components under the different light source which is new due to the different shape. This indicates that we can reproduce the gloss component under the new light source. The reproduced gloss is synthesized with the diffuse component, where the specular component is removed by the image inpainting technique [38].

4.2 Results

Figure 13 shows the result of four samples, for which parameter a for the reflectance property is estimated from the edge of the specular reflectance components, and SR-PSF is convolved with a different light source. Figure 14 shows the result of the reproduction under fluorescent illumination. The spread of gloss is wider in the order of (a), (b), (c), (d).

5. Conclusion

In this research, we performed an estimation of the reflectance property from refocused images under limited conditions. It is necessary to consider various conditions, such as the distance between a

light source and an object surface, the distance between Lytro and the object surface, and the types of light sources. We also assumed that the shape of the object is planar. If the object is not planar, it is necessary to consider the curvature and transform the geometry into a planar shape. In this research, we analyzed the change of gloss in the spatial domain. The frequency domain is expected to be used as implemented by Romeiro et al. [21] because it is not necessary to consider the inclusion of the edge pattern. Perturbation on the edge is treated as noise in this research. However, the meso-structure is included in this noise pattern [22,27]. Therefore, by analyzing the noise, it is expected that the meso-structure can be measured, and in gloss reproduction, it is necessary to consider the shape and the meso-structure of the surface for accurate reproduction.

Acknowledgment

Norimichi Tsumura would like to thank to Dr. Mohit Gupta and Prof. Shree K. Nayar for my stay at Columbia University and for their productive discussions.

REFERENCES

1. Spitzer, H., and Semo, S., "Color constancy: A biological model and its application for still and video images", Pattern Recognit., vol. 35, pp. 1645–1659, (2002).
2. Hsu, E., Mertens, T., Paris, S., Avidan, S., and Durand, F., "Light mixture estimation for spatially varying white balance", ACM Transactions on Graphics, 27(3), pp. 1–7, (2008).
3. Gijsenij, A., Lu, R., and Gevers, T., "Color constancy for multiple light sources", Image Processing, IEEE Transactions on, 21(2), pp. 697–707, (2012).
4. Fleming, R., Dror, R., Adelson, E., "Real-world illumination and the perception of surface reflectance properties", Journal of Vision, 3, 5, pp. 347–368, (2003).
5. Matusik, W., Pfister, H., Brand, M., and McMillan, L., "Efficient Isotropic BRDF Measurement", Proc. Eurographics Symposium on Rendering, pp. 241–247, (2003).
6. Ezra, M.B., Wang, J., Wilburn, B., Li, X., and Ma, L., "An LED-only BRDF measurement device", IEEE conference on computer vision and pattern recognition, pp. 1–8, (2008).
7. Gardner, A., Tchou, C., Hawkins, T., and Debevec, P., "Linear Light Source Reflectometry", ACM Transactions on Graphics 22, 3, pp. 749–758, (2003).
8. Wang, J., Zhao, S., Tong, X., Snyder, J., and Guo, B., "Modeling Anisotropic Surface Reflectance with Example-Based Microfacet Synthesis", ACM Transactions on Graphics, pp. 1–9, (2008).
9. Ren, P., Wang, J., Snyder, J., Tong, J. X., and Guo, B., "Pocket Reflectometry", ACM Transactions on Graphics 30, 4, pp. 45:1–45:10, (2011).
10. Alldrin, N., Zickler, T., and Kriegman, D., "Photometric Stereo with Non-Parametric and Spatially-Varying Reflectance", Vision and Pattern Recognition, pp. 1–8, (2008).
11. Ghosh, A., Chen, T., Peers, P., Wilson, C. A., and Debevec, P., "Circularly Polarized Spherical Illumination Reflectometry", ACM Transactions on Graphics 29, pp. 162:1–162:12, (2010).
12. Ghosh, A., Fyffe, G., Tunwattanapong, B., Busch, J., Yu X., and Debevec, P., "Multiview Face Capture using Polarized Spherical Gradient Illumination", Eurographics Symposium on Rendering, Proc. SIGGRAPH Asia, pp. 129:1–129:10, (2011).

13. Makino, T., Tsumura, N., Takase, K., Homma, R., Nakaguchi, T., Ojima, N., and Miyake, Y., "Development of the Measurement System for Facial Physical Properties with the Short-Distance Lighting", Journal of Imaging Science and Technology, 53, 6, pp. 605011–605019, (2009).
14. Hasegawa, T., Tsumura, N., Nakaguchi, T., and Iino, K., "Photometric approach to surface reconstruction of artist paintings", Journal of Electronic Imaging 20(1), 013006-1-11 (2011).
15. Holroyd, M., Lawrence, J., and Zickler, T., "A Coaxial Optical Scanner for Synchronous Acquisition of 3D Geometry and Surface Reflectance", ACM Transactions on Graphics 29, 4, pp. 99:1–99:12, (2010).
16. Dong, Y., Snyder, J., Tong, X., Snyder, J., Lan, Y., Benezra M., and Guo, B., "Manifold Bootstrapping for SVBRDF Capture", ACM Transactions on Graphics 29, 4, pp. 98:1–98:10, (2010).
17. Schwartz, C., Weinmann, M., Ruiters, R., Zinke A., and Sarlette, R., "Capturing Shape and Reflectance of Food", Proc. SIGGRAPH Asia, (2011).
18. Naik, N., Zhao, S., Velten, A., Raskar, R., and Bala, K., "Single View Reflectance Capture using Multiplexed Scattering and Time-of-flight Imaging", Proc. SIGGRAPH Asia, (2011).
19. Aittala, M., Weyrich, T., and Lehtinen, J., "Practical SVBRDF Capture in the Frequency Domain", ACM Transactions on Graphics 32, 4, (2013).
20. Romeiro, F., Vasilyev, Y., and Zickler, T., "Passive Reflectometry", Proc. ECCV, pp. 859–872, (2008).
21. Romeiro, F., and Zickler, T., "Blind Reflectometry", Proc. ECCV, pp. 45–58, (2010).
22. Wang, C.-P., Snavely, N., and Marshner, S., "Estimating Dual-scale Properties of Glossy Surfaces from Step-edge Lighting", ACM Transactions on Graphics 30, 6, pp. 172:1–172:12, (2011).
23. Inoue S., and Tsumura, N., "Point Spread Function of Specular Reflection and Gonio-reflectance Distribution", J. Imaging Sci. Technol., (2015) (in press).
24. Inoue, S., Kotori, Y., and Takishiro, M., "Measurement Method for PSF of Paper on Specular Reflection Phenomenon (Part I) ", Japan Tappi Journal, 66, 8, pp. 871–886, (2012).
25. Inoue, S., Kotori, Y., and Takishiro, M., "Measurement Method for PSF of Paper on Specular Reflection Phenomenon (Part II) ", Japan Tappi Journal, 66, 12, pp. 1425–1434, (2012).
26. LYTRO incorporated, Lytro camera, https://www.lytro.com/

27. Raytrix GmbH company, Raytrix-R11 3D Light Field camera, http://www.raytrix.de/

28. Venkataraman, K., Lelescu, D., Duparré, J., McMahon, A., Molina, G., Chatterjee, P. and Mullis, R., "An Ultra-Thin High Performance Monolithic Camera Array", ACM Transactions on Graphics 32, 5, (2013).

29. Perwa, C., and Wietzke, L., "Single lens 3D-camera with extended depth-of-field", SPIE Electronic Imaging, pp. 829108–829108, (2012).

30. Levoy, M., and Hanrahan, P., "Light Field Rendering", Proc. 23rd Annual Conference on Computer Graphics and Interactive Techniques, pp. 31–42, (1996).

31. Ng, R., Levoy, M., Bre'dif, M., Duval, G., Horowitz, M., and Hanrahan, P., "Light Field Photography with a Hand-held Plenoptic Camera", Computer Science Technical Report CSTR, volume 2, (2005).

32. Ng, R., "Fourier Slice Photography", ACM Transactions on Graphics (TOG), volume 24(3), pp. 735–744, (2005).

33. Tanida, J., Kumagai, T., Yamada, K., Miyatake, S., Ishida, K., Morimoto, T., Kondou, N., Miyazaki, D., and Ichioka, Y., "Thin observation module by bound optics (TOMBO): concept and experimental verification", Applied Optics, volume 40(11), pp. 1806–1813, (2001).

34. Inoue, S., Tsumura, N., and Miyake, Y., "Measuring MTF of Paper by Sinusoidal Test Pattern Projection", J. Imaging Sci. Technol., 41, 6, pp. 657–661, (1997).

35. Rogers, G.L., "Measurement of the modulation transfer function of paper", Appl. Opt., 37, 31, pp. 7235–7240, (1998).

36. Baba, K., Takano, R., Inoue, S., Miyata, K., and Tsumura, N., "Simulation of Paper Gloss by Point Spread Function of Specular Reflection", Proc. CIC, pp. 216–220, (2012).

37. Baba, K., Takano, R., Inoue, S., and Tsumura, N., "Reproducing Gloss Unevenness on Printed Paper based on the Measurement and Analysis of Mesoscopic Facet", J. Imaging Sci. Technol. 58(3): 030501-1–030501-6, (2014).

38. Bertalmio, M., Sapiro, G., Caselles, V., and Ballester, C., "Image inpainting", SIGGRAPH '00 Proc. 27th Annual Conference on Computer Graphics and Interactive Techniques, pp. 417–424, (2000).

Figure captions

Figure 1. Change of blurriness under different focus positions.

Figure 2. Apparatus used to measure the SR-PSF.

Figure 3. SR-PSF for the six kinds of samples with different gloss.

Figure 4. Cross sections of SR-PSF for the six kinds of samples.

Figure 5. Parameter a for the six kinds of samples.

Figure 6. Geometry of light source, camera, and analysis area to estimate the reflectance property.

Figure 7. Observed values are convolution among shape of light source, SR-PSF, PSF caused by focus. PSF caused by focus can be controlled in the light field camera.

Figure 8. Experimental setup.

Figure 9. Edge slopes at various positions of focus. The maximum slope value is used as parameter a.

Figure 10. Observed convolved value between edge function and SR-PSF.

Figure 11. Measured and estimated parameter a for the six kinds of samples.

.

Figure 12. Flow of the proposed method for gloss reproduction.

Figure 13. Captured image and estimated SR-PSFs with parameter a for four kinds of samples.

Figure 14. Captured and simulated images for gloss reproduction of four kinds of samples.

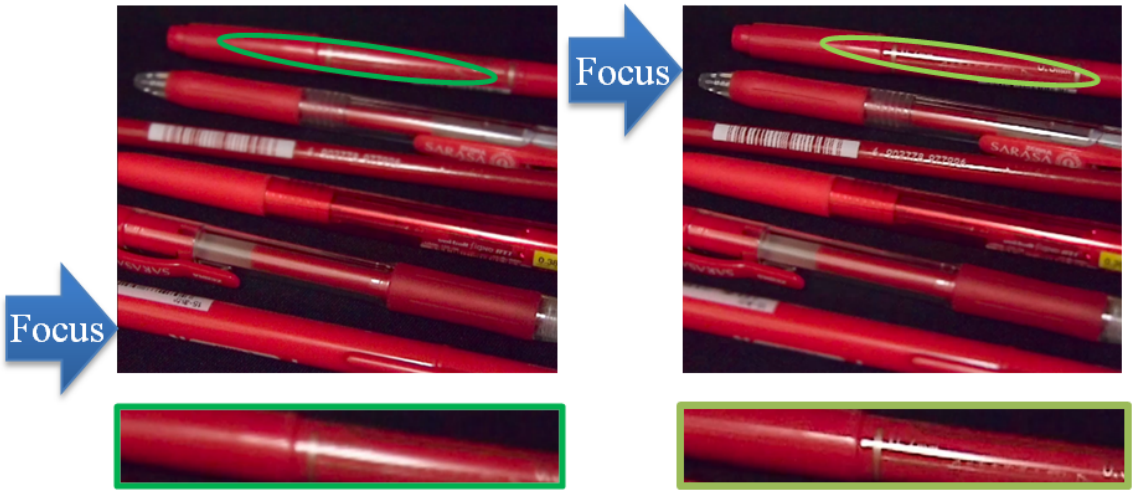

Figure 1.

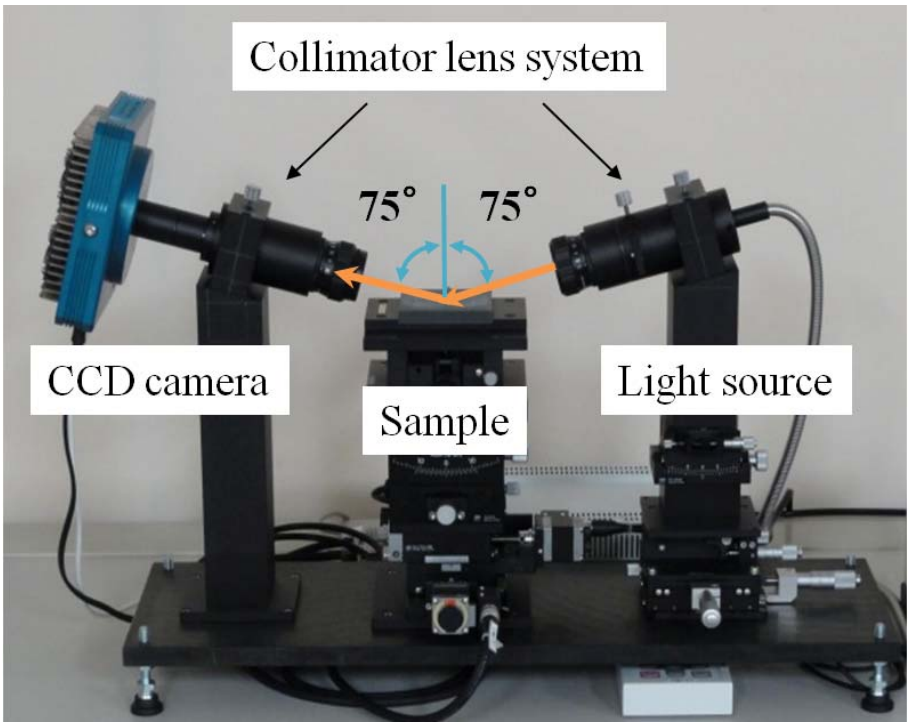
Collimator lens system
75°
75°
CCD camera
Sample
Light source

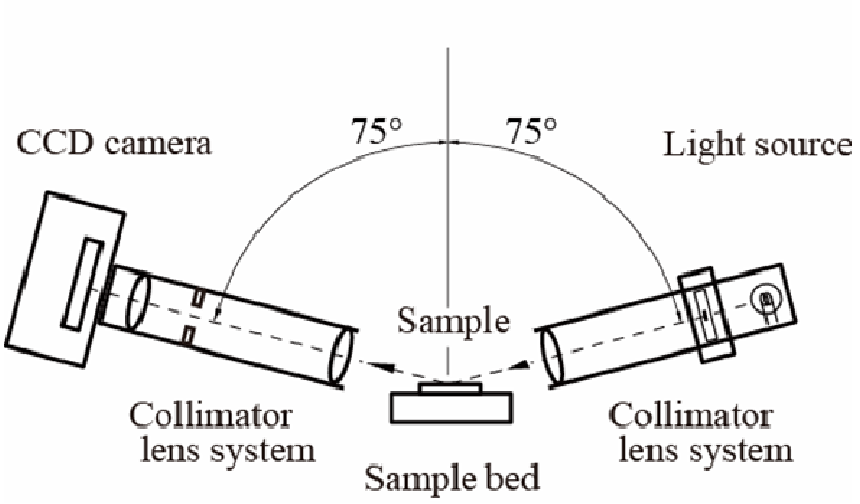
CCD camera
75°
75°
Light source
Sample
Collimator lens system
Collimator lens system
Sample bed

Figure 2.

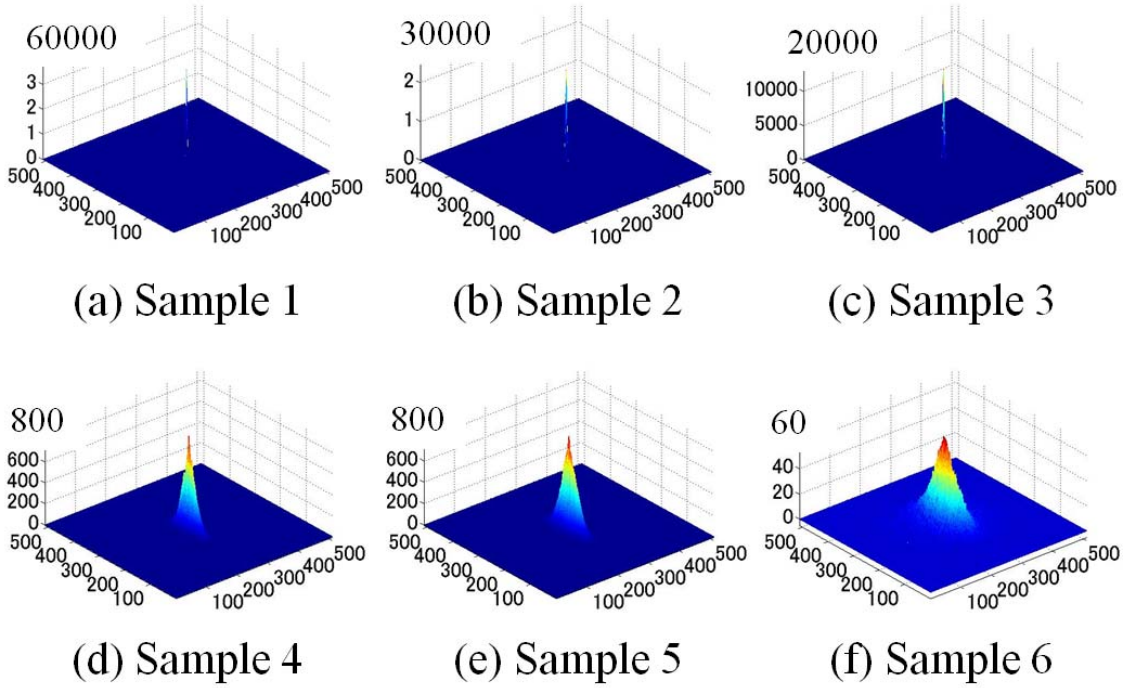
60000
30000
20000
(a) Sample 1
(b) Sample 2
(c) Sample 3
800
800
60
(d) Sample 4
(e) Sample 5
(f) Sample 6

Figure 3.

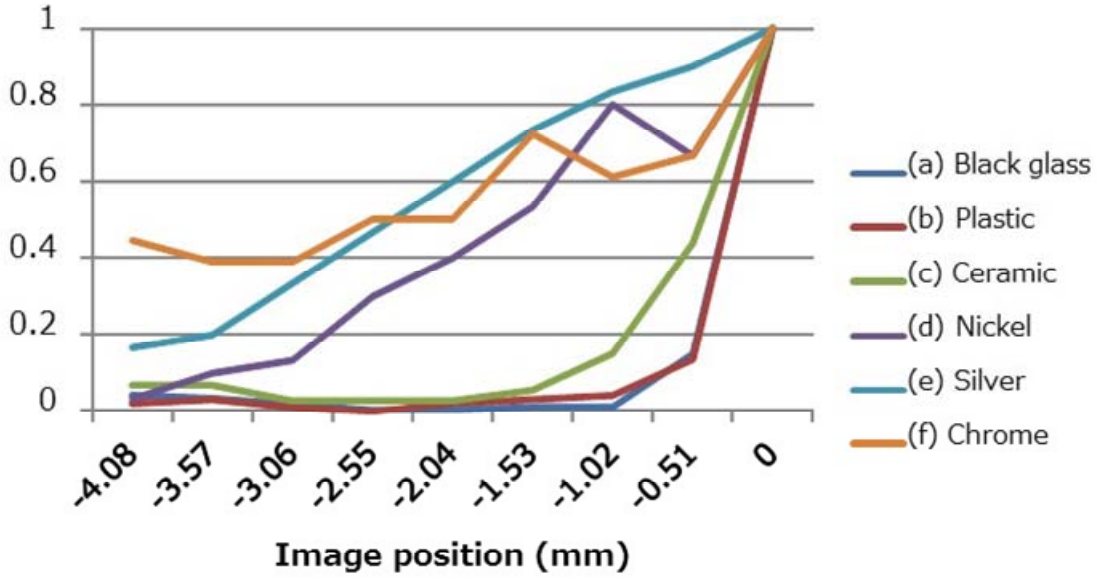
1
0.8
0.6
0.4
0.2
0
-4.08
-3.57
-3.06
-2.55
-2.04
-1.53
-1.02
-0.51
0
Image position (mm)
(a) Black glass
(b) Plastic
(c) Ceramic
(d) Nickel
(e) Silver
(f) Chrome

Figure 4.

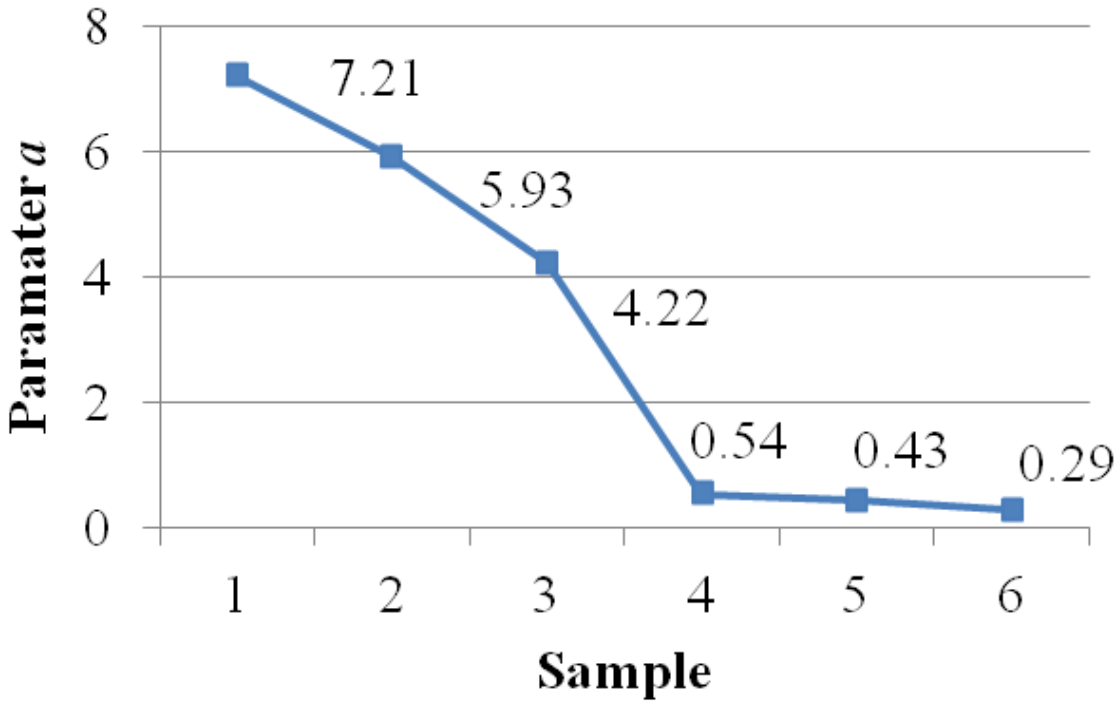

Figure 5.

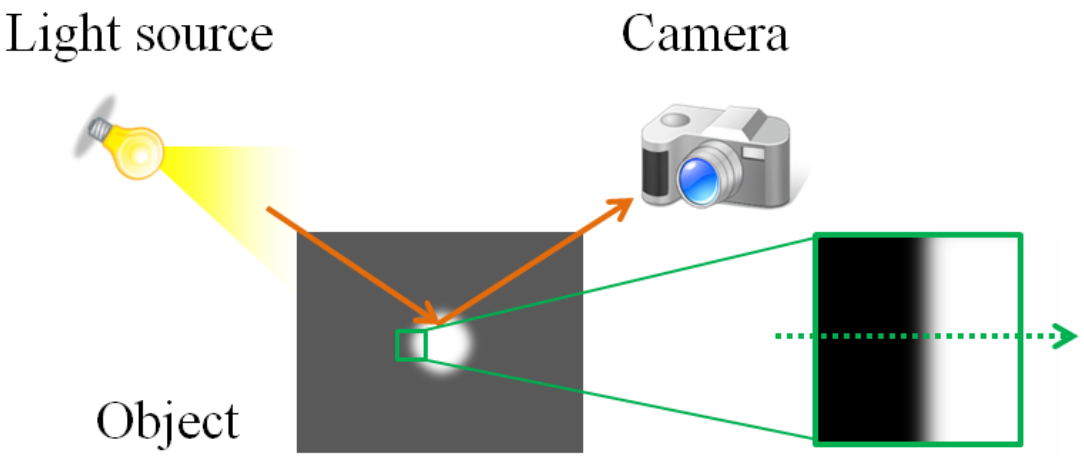

Figure 6.

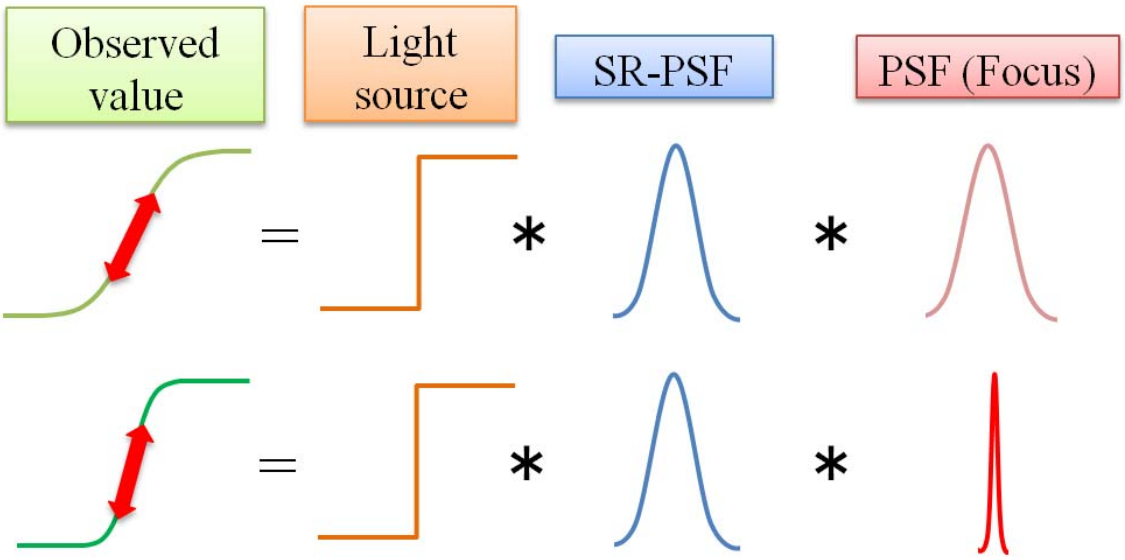

Figure 7.

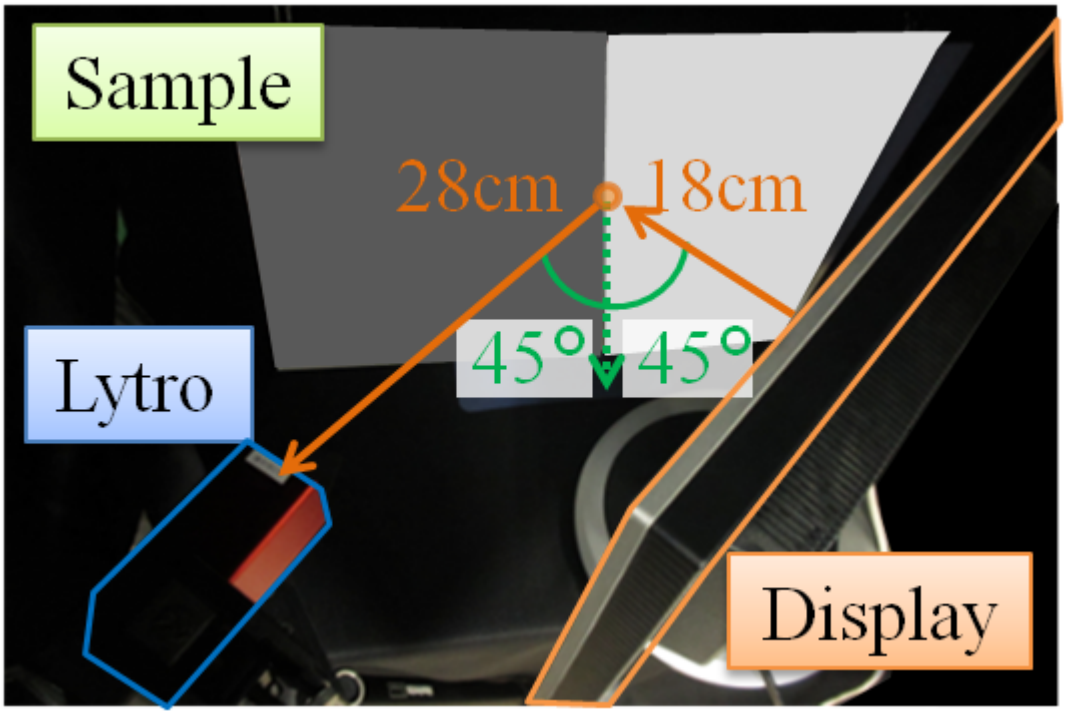

Figure 8.

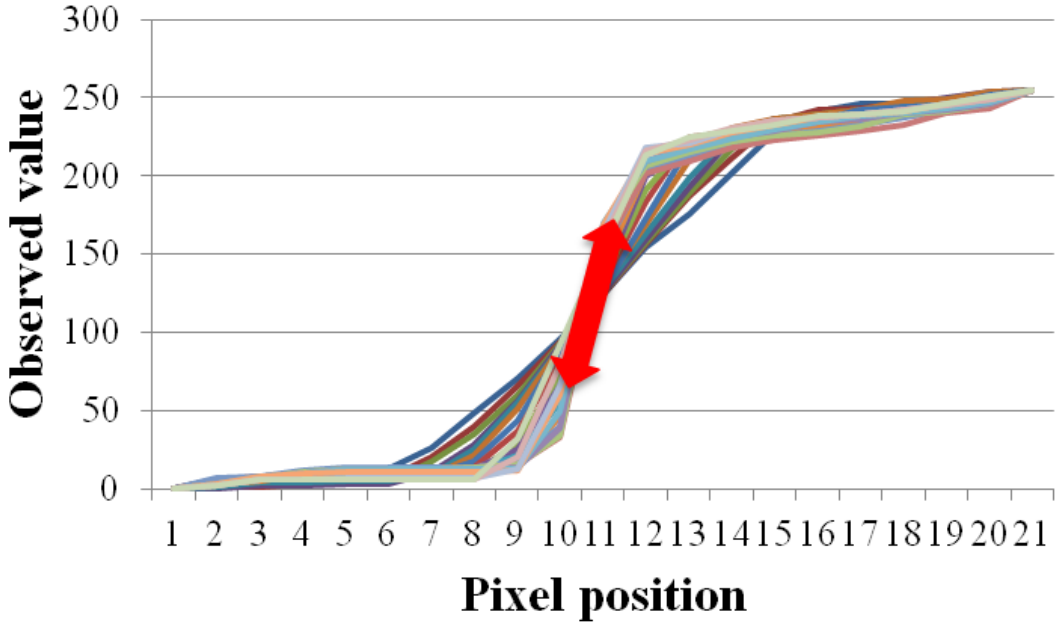
Observed value
300
250
200
150
100
50
0
1 2 3 4 5 6 7 8 9 10 11 12 13 14 15 16 17 18 19 20 21
Pixel position

Figure 9.

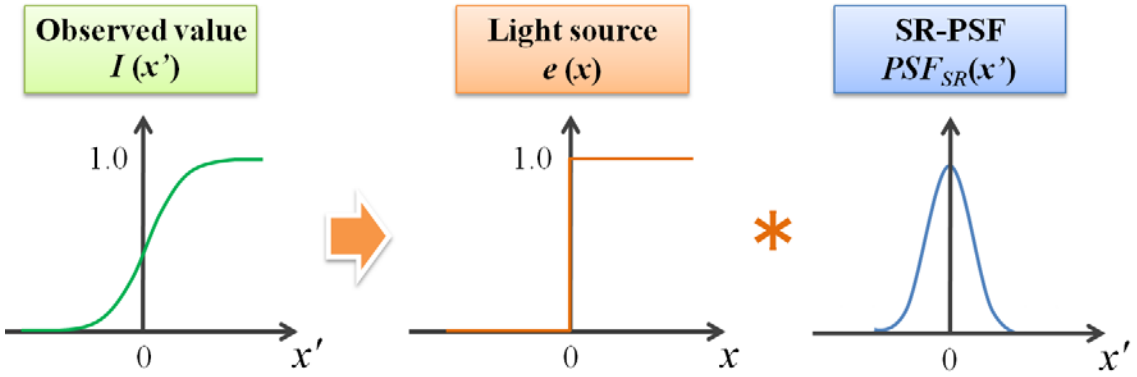

Figure 10.

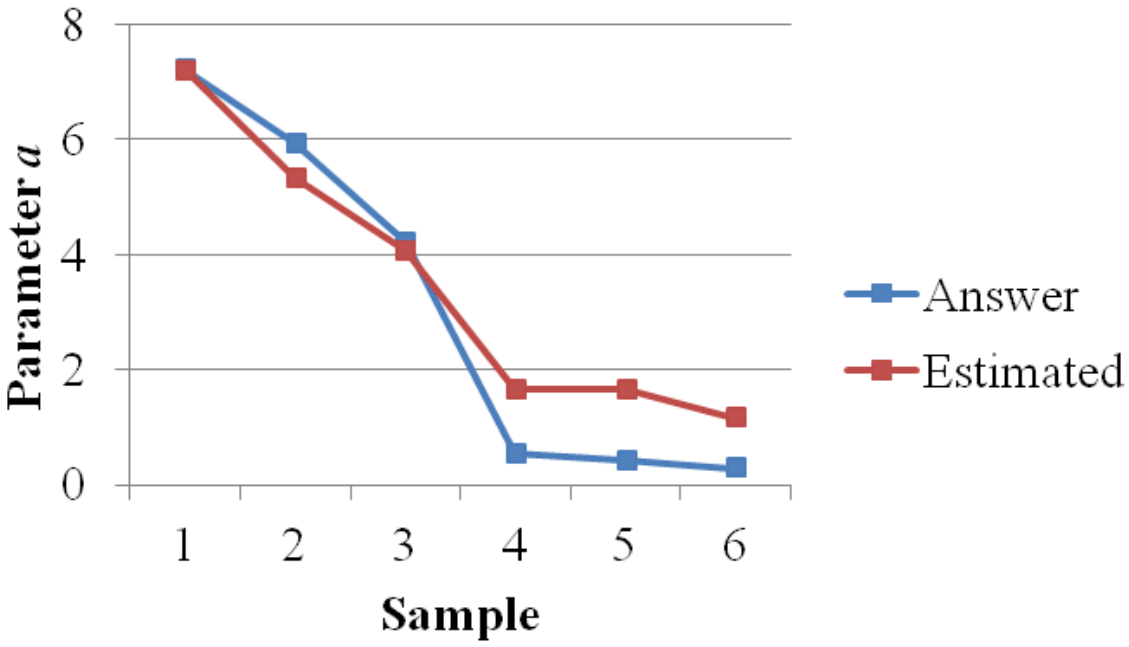

Figure 11.

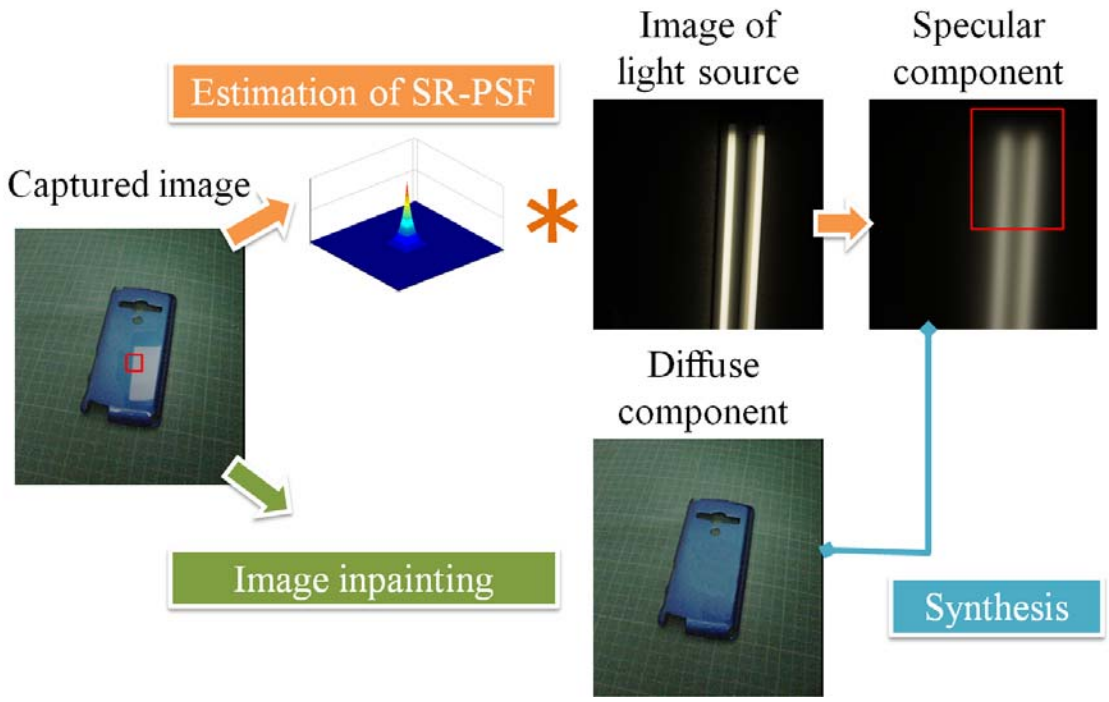
Image of
light source
Specular
component
Estimation of SR-PSF
Captured image
Diffuse
component
Image inpainting
Synthesis

Figure 12.

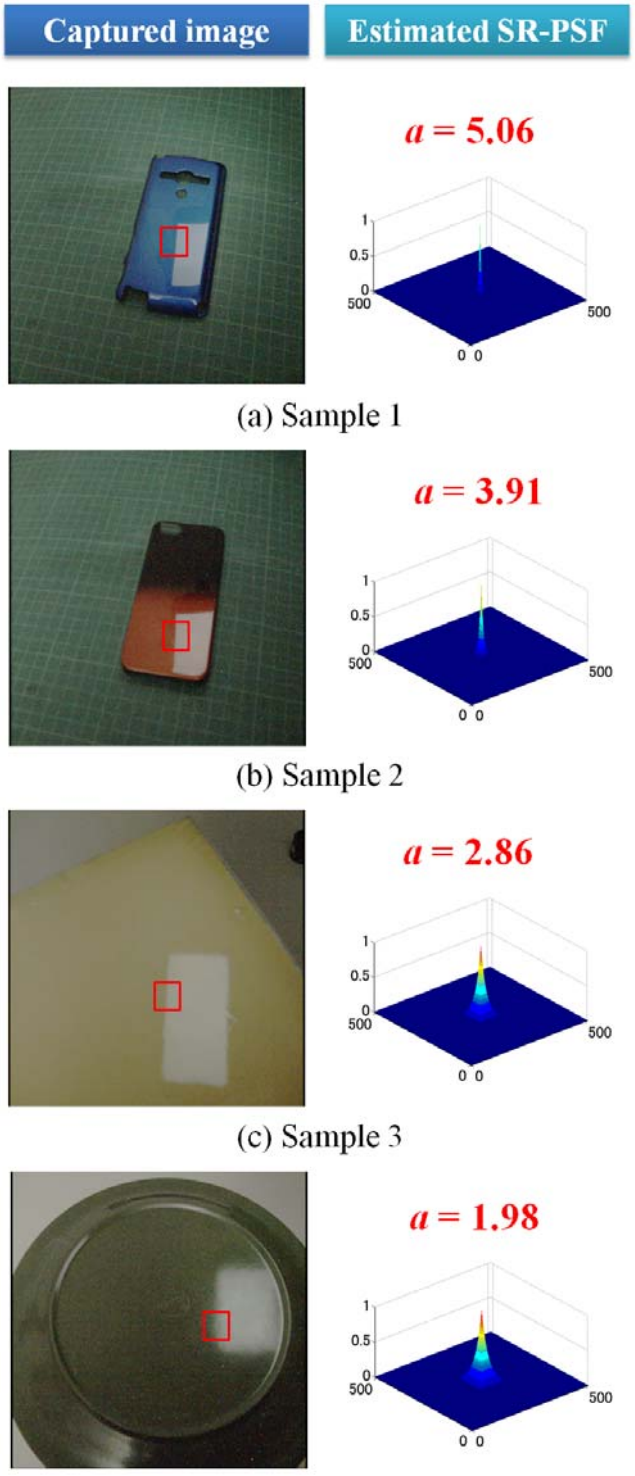
Captured image
Estimated SR-PSF
a = 5.06
1
0.5
0
500
500
0 0
(a) Sample 1
a = 3.91
1
0.5
0
500
500
0 0
(b) Sample 2
a = 2.86
1
0.5
0
500
500
0 0
(c) Sample 3
a = 1.98
1
0.5
0
500
500
0 0
(d) Sample 4

Figure 13.

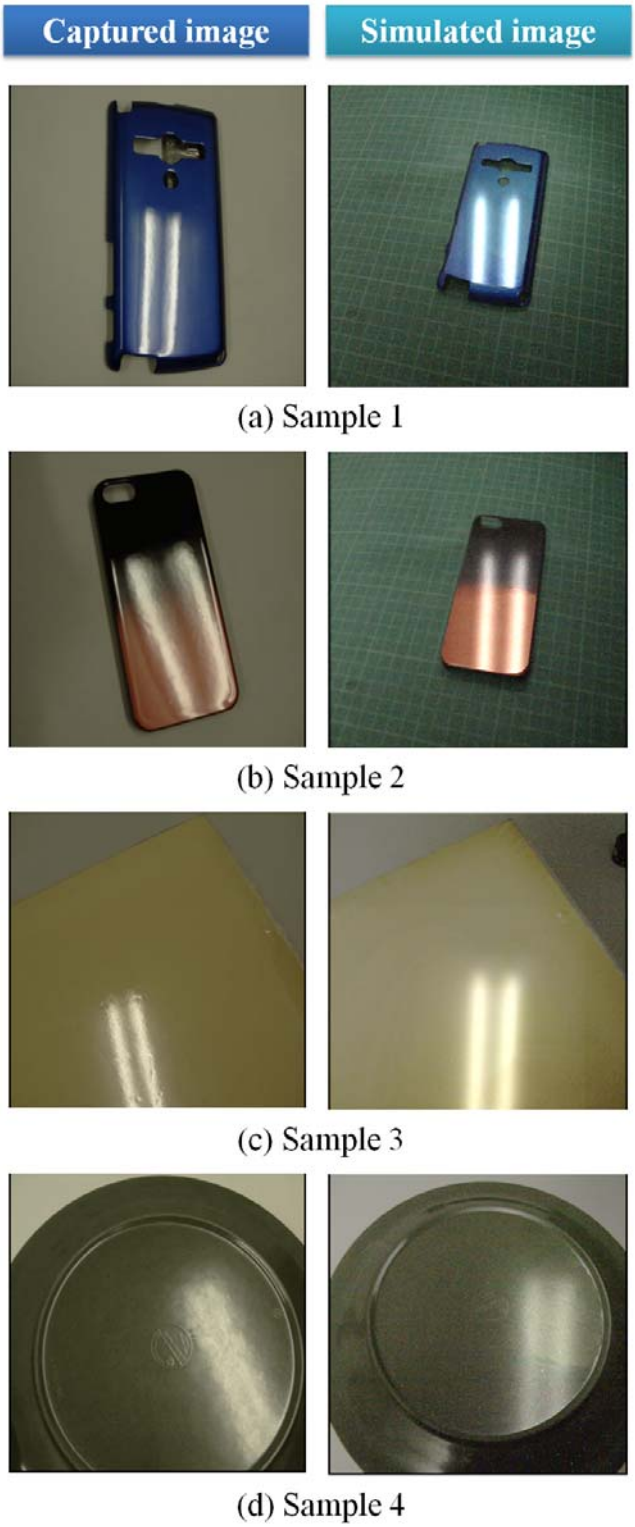
Captured image
Simulated image
(a) Sample 1
(b) Sample 2
(c) Sample 3
(d) Sample 4

Figure 14.